

Article

Silica Nanoparticles-Induced Lysozyme Crystallization: Effects of Particle Sizes

Yuxiao Zhang , Xuntao Jiang, Xia Wu, Xiaoqiang Wang, Fang Huang, Kefei Li, Gaoyang Zheng, Shengzhou Lu, Yanxu Ma, Yuyu Zhou and Xiaoxi Yu *

State Key Laboratory of Heavy Oil Processing, College of Chemistry and Chemical Engineering, China University of Petroleum (East China), Qingdao 266580, China

* Correspondence: yuxiaoxi@upc.edu.cn; Tel.: +86-17606393651

Abstract: This study aimed to explore the effects of nucleate agent sizes on lysozyme crystallization. Silica nanoparticles (SNP) with four different particle sizes of 5 nm, 15 nm, 50 nm, and 100 nm were chosen for investigation. Studies were carried out both microscopically and macroscopically. After adding SNP, the morphological defects of lysozyme crystals decreased, and the number of crystals increases with the size of the SNP. The interaction between SNP and lysozyme was further explored using UV spectroscopy, fluorescence spectroscopy, and Zeta potential. It was found that the interaction between SNP and lysozyme was mainly electrostatic interaction, which increased with the size of SNP. As a result, lysozyme could be attracted to the surface of SNP and aggregated to form the nucleus. Finally, the activity test and circular dichroism showed that SNP had little effect on protein secondary structure.

Keywords: nanoparticle size; lysozyme crystallization; electrostatic interaction



Citation: Zhang, Y.; Jiang, X.; Wu, X.; Wang, X.; Huang, F.; Li, K.; Zheng, G.; Lu, S.; Ma, Y.; Zhou, Y.; et al. Silica Nanoparticles-Induced Lysozyme Crystallization: Effects of Particle Sizes. *Crystals* **2022**, *12*, 1623. <https://doi.org/10.3390/cryst12111623>

Academic Editors: Jingxiang Yang and Xin Huang

Received: 31 October 2022

Accepted: 9 November 2022

Published: 12 November 2022

Publisher's Note: MDPI stays neutral with regard to jurisdictional claims in published maps and institutional affiliations.



Copyright: © 2022 by the authors. Licensee MDPI, Basel, Switzerland. This article is an open access article distributed under the terms and conditions of the Creative Commons Attribution (CC BY) license (<https://creativecommons.org/licenses/by/4.0/>).

1. Introduction

Single crystal X-ray diffraction technology [1] is a primary technical means to analyze the atomic-level structure of biological macromolecules. The successful application of X-ray [2] crystallography in determining the 3-D structure of proteins relies on the cultivation of high-quality protein crystals [3–5]. However, protein crystallization is more complicated than small molecules due to the complexity and instability of protein molecules. Therefore, conducting in-depth research on the crystallization process of proteins is necessary.

Similar to small molecules, the nucleation process of protein crystallization [6,7] goes in two ways: homogeneous nucleation and heterogeneous nucleation [8]. Kordon-skaya et al. [9–11] studied the growth of tetragonal crystals under homogeneous nucleation. It was found that lysozyme forms oligomers prior to crystal formation, which may be intermediates and can serve as growth units in crystal growth. Due to a high potential barrier in protein solution is high enough, which easily causes precipitates and is limited in low protein concentration systems. In contrast, when foreign substances exist as nucleating agents in the crystallization solution, the nucleation potential barrier will be significantly reduced due to protein adherence to the nucleating agent. As a result, heterogeneous nucleation could occur at relatively low protein concentrations. Therefore, it is beneficial for improving the quality of protein crystals and obtaining better diffraction data.

Nanomaterials refer to materials that have at least one dimension of nanometer size (1–100 nm) in three-dimensional space. Due to their excellent biocompatibility, nanomaterials have attracted much attention in studying the heterogeneous nucleation of proteins. Gold nanoparticles [12], platinum nanoparticles [13] and functionalized carbon nanoparticles [14] were proven to be effective in promoting protein crystallization and increasing crystal quality. Another commonly studied nanomaterial was silica nanoparticles (SNP),

which were also confirmed to assist protein crystallization. Compared with other nanomaterials, SNP is cheaper and easier to synthesize. Therefore, SNP has better application potential for the research and industrialization of protein crystallization.

The size of nanoparticles is an important factor affecting its properties. Peukert et al. carried out lysozyme crystallization using silica nanoparticles (SNP) ranging from 10 to 200 nm. The addition of SNP brought about a clear extension in the crystallization window, especially when larger seed particles were used [12]. Interestingly, the work of Delmas investigated the effect of silica particles with sizes from 230 nm to 698 nm and found that the optimal nucleation occurred when particles sizes were 432 nm [15]. Up to now, the mechanism of SNP size on inducing an effect on protein crystallization is still unclear. In addition, the different preparation methods of SNP [16,17] will also lead to differences in their surface properties, affecting the interaction between SNP and proteins. Therefore, it is necessary to deeply explore the effect of silica with different particle sizes on protein crystallization.

In this work, SNP with sizes of 5 nm, 15 nm, 50 nm, and 100 nm were utilized as the nucleating agent, and lysozyme was chosen as the model protein. The influences of SNP sizes on lysozyme crystallization were studied using crystal morphology in the first place. To further reveal the intermolecular interactions between SNP and lysozyme, UV spectroscopy, fluorescence spectroscopy, and Zeta potential were applied. Finally, activity tests and circular dichroism were carried out to determine the effect of SNP on the secondary structure and function of proteins.

2. Materials and Methods

2.1. Materials

Hen egg white lysozyme (HEWL) with a purity of 99% was purchased from Beijing Solarbio Technology of China (Beijing, China) and used directly without further purification. *Micrococcus lysodeikticus* (ATCC No. 4698, Manassas, VA, USA), used for the lysozyme activity assay, was purchased from Sigma-Aldrich. Analytical grade reagents, such as acetic acid, sodium hydrate, sodium chloride, and anhydrous sodium acetate, were purchased from Sinopharm Chemical Reagent Co. Ltd. (Shanghai, China). SNP of different sizes were purchased from Shanghai Jiute Nano Material Technology Co. Ltd. (Shanghai, China). The sizes of SNP were evaluated using transmission electron microscopy (See Supplementary Materials Figure S1). The information of SNP is shown in Table 1. Ultrapure water was used in all experiments.

Table 1. Properties of the SNP used in this investigation.

Particle Size, nm	C _{SiO₂} , mg/mL	ρ , g/mL	wt, %	pH
5	10	1.13	20	3–5
15	10	1.21	30	9–10
50	10	1.13	20	9–10
100	10	1.13	20	9–10

2.2. Lysozyme Crystallization

Lysozyme crystallization experiments were carried out in 96-well plates. The concentration of each crystallization solution contained: 15 or 20 mg/mL lysozyme and 3 wt.% sodium chloride. SNP with four different sizes were used as the nucleating agent, respectively, and the concentration was kept at 1 mg/mL. All materials were dissolved in a pH = 4.5, 0.05 M sodium acetate buffer. After gentle mixing, the 96-well plates were sealed with parafilm to prevent evaporation and placed in a refrigerator at T = 4 °C. After every 24 h, the plates were taken out and analyzed using a microscope.

2.3. UV Spectroscopy Experiment

UV spectroscopy was carried out using a lysozyme and SNP solution mixture. The UV spectrophotometer was preheated for 30 min before measuring. At ambient temperature, a

UV cell with a 1 cm light path was selected to measure the UV absorption spectrum of the prepared solution in the 200–800 nm band. Sodium acetate buffer was used for calibration before measuring.

2.4. Fluorescence Spectroscopy Experiment

The samples containing 10 mg/mL lysozyme and SNP with different sizes were incubated for 24 h. Afterward, the solution was added to a 1 cm light path cuvette. The scan mode was set to Emission, and the data mode was selected as Fluorescence [18]. The fluorescence emission spectrum of lysozyme was carried out with an excitation wavelength of 280 nm and a slit of 3 nm.

2.5. Zeta Potentials of Lysozyme and SNP

Zeta potential was measured for both lysozyme and SNP solutions. The concentrations were all 5 mg/mL. A DTS1060 sample cell was used for the measurement. The measurement parameters were the Zeta interface and manual measurement, respectively. The measurements were repeated several times until the data became stable.

2.6. Enzyme Activity Experiment

Lysozyme activity was measured using *Micrococcus lysodeikticus* as the substrate. A cuvette with an optical path length of 1 cm and a volume of 4 mL was used. A 2.5 mL bacterial suspension with an absorbance value (at 450 nm) of about 1.3 was added to the cuvette. Then, 200 μ L of lysozyme solution (0.1 mg/mL) was added to the cuvette and mixed immediately. The absorbance values A_1 and A_2 at 450 nm at 1 min and 2 min were recorded at 25 °C. The activity of lysozyme (0.1 mg/mL) and SNP solutions with different particle sizes was also evaluated.

The enzymatic activity E_A was calculated by the following formula [19]:

$$E_A = \frac{\Delta E_{450\text{nm}}}{0.001 \times E_W} \quad (1)$$

where $\Delta E_{450\text{nm}}$ is the change of absorbance per minute at 450 nm, namely $|A_1 - A_2|$; E_W is the mass of the original enzyme contained in the 0.5 mL detection enzyme solution, mg; 0.001 is a unit in which the absorbance drops; and E_A is the specific activity of the enzyme, with a unit of U/mg.

3. Results and Discussion

3.1. Effect of SNP Sizes on Lysozyme Crystal Morphology

The microscopy images of the lysozyme crystals obtained are shown in Figure 1. Lysozyme crystals were analyzed at different times. Within 24 h, the solution without SNP did not form crystals (Figure 1a). While in crystallization solutions with SNP, tiny crystals formed (Figure 1b–e). When the crystallization time was extended to 48 h and 72 h, the crystals in solutions containing SNP continued to grow (Figure 1g–j,l–o). No crystals could be observed under homogeneous nucleation conditions until 72 h (Figure 1k).

It can be further seen from Figure 1 that the number of crystals changed regularly with the SNP sizes. The numbers of crystals were estimated by image processing and are displayed in Figure 2. The number of crystals increased rapidly within 48 h. The addition of SNP could promote lysozyme nucleation, which agrees with the work of Yamazaki et al. [20]. After 48 h, the increase in the number of crystals slowed down due to the decrease in supersaturation. During the crystallization time investigated, the number of crystals increased with the size of SNP. The size distribution of lysozyme crystals after 48 h and 72 h was estimated and is shown in Figures S2 and S3. It can be found that the particle size of SNP showed no significant effect on the size of lysozyme crystals within 48 h. After 72 h, the crystal size of lysozyme decreased with the increase in SNP size, due to the larger supersaturation consumed. Lysozyme crystallization was further carried out

at protein concentrations of 20 mg/mL with SNP of different sizes. A similar phenomenon was observed, as shown in Figure 3.

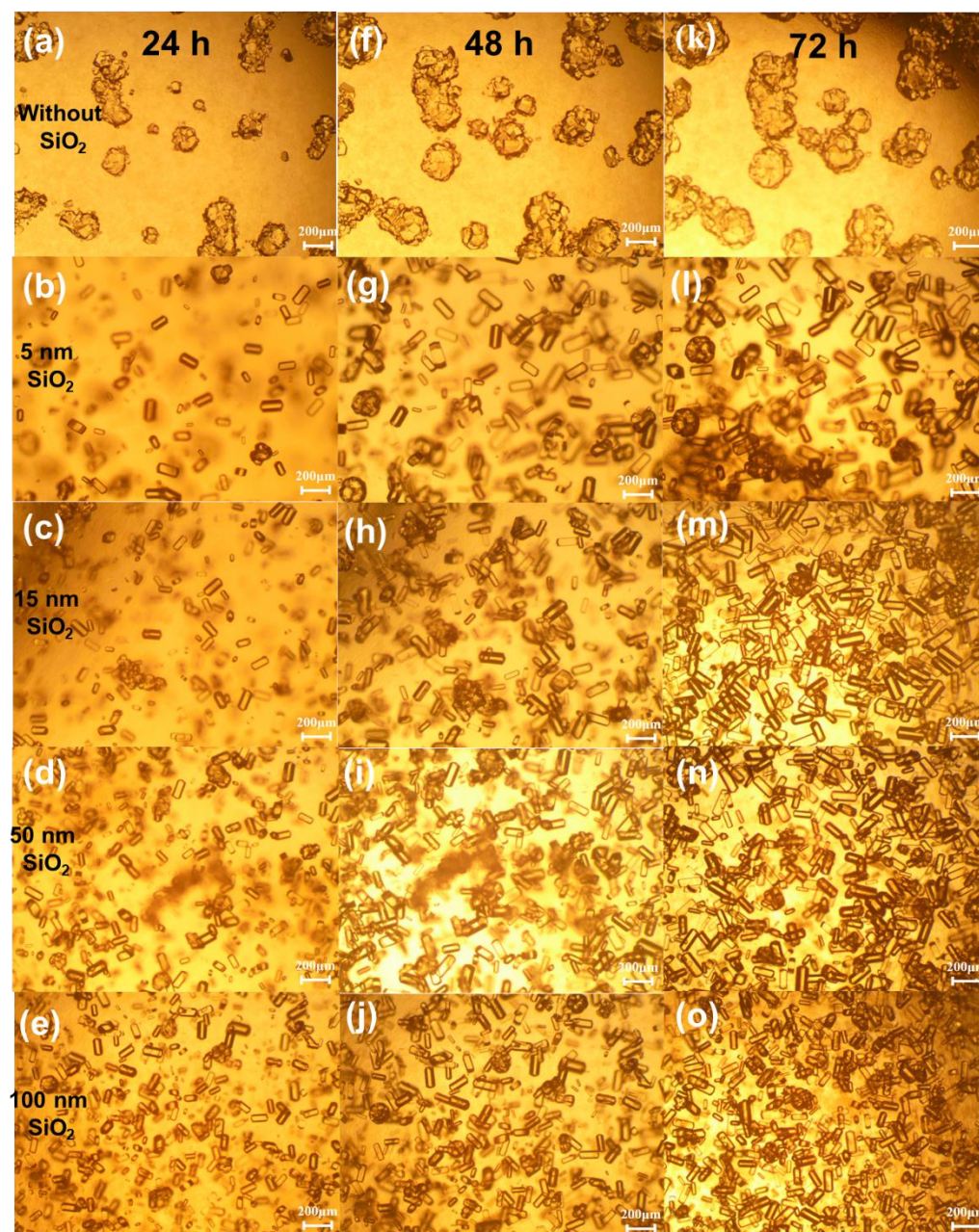


Figure 1. Microscopy photos of crystals obtained with SNP of different sizes. Conditions: 0.05 M, pH 4.5 sodium acetate buffer solution, 3 wt.% sodium chloride, 15 mg/mL lysozyme at 4 °C. Scale bar: 200 μm . (a): Crystal micrograph obtained under 24 h without SiO_2 ; (b): Crystal micrograph obtained at 24 h with 1 mg/mL 5 nm SiO_2 ; (c): Crystal micrograph obtained at 24 h with 1 mg/mL 15 nm SiO_2 ; (d): Crystal micrograph obtained at 24 h with 1 mg/mL 50 nm SiO_2 ; (e): Crystal micrograph obtained at 24 h with 1 mg/mL 100 nm SiO_2 ; (f): Crystal micrograph obtained under 48 h without SiO_2 ; (g): Crystal micrograph obtained at 48 h with 1 mg/mL 5 nm SiO_2 ; (h): Crystal micrograph obtained at 48 h with 1 mg/mL 15 nm SiO_2 ; (i): Crystal micrograph obtained at 48 h with 1 mg/mL 50 nm SiO_2 ; (j): Crystal micrograph obtained at 48 h with 1 mg/mL 100 nm SiO_2 ; (k): Crystal micrograph obtained under 72 h without SiO_2 ; (l): Crystal micrograph obtained at 72 h with 1 mg/mL 5 nm SiO_2 ; (m): Crystal micrograph obtained at 72 h with 1 mg/mL 15 nm SiO_2 ; (n): Crystal micrograph obtained at 72 h with 1 mg/mL 50 nm SiO_2 ; (o): Crystal micrograph obtained at 72 h with 1 mg/mL 100 nm SiO_2 .

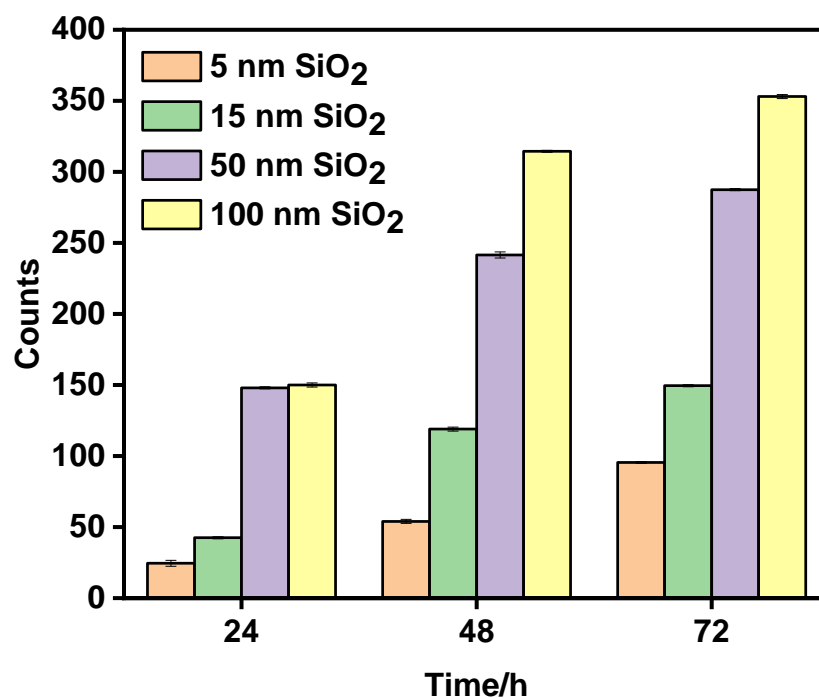


Figure 2. Histogram of the number of crystals with SNP of different sizes as a function of time. Conditions: 0.05 M, pH 4.5 sodium acetate buffer solution, 3 wt.% sodium chloride, 15 mg/mL lysozyme at 4 °C.

In this work, lysozyme crystallization was carried out at 4 °C, in sodium acetate buffer solution near pH = 4.5 with 3 wt.% NaCl. The crystal formed at such conditions is considered to exhibit a tetragonal morphology [21–24]. As stated in other works, no significant effect on the structure of lysozyme crystals was discovered when nanoparticles such as gold particles or carbon quantum dots (GQDs) were used as nucleating agents [12,25]. Therefore, it is speculated here that the addition of nanoparticles may not alter the lysozyme crystal assembly process and that the lysozyme crystals obtained belong to a tetragonal morphology.

As shown in Figures 1 and 3, the crystals obtained with SNP are longer in the 110-face. Forsythe et al. [26] have experimentally demonstrated that the growth of different faces in lysozyme crystals is strongly dependent on the supersaturation of the protein, resulting in changes in the shape of the crystals. The 110-face of the lysozyme crystal grows faster with the increase in supersaturation. As further discovered in Figure S4, some agglomerates could be observed in solutions containing SNP of larger particle sizes and lysozyme. Sun et al. [27] found out that lysozyme could adsorb on SNP and the adsorption was related to the surface curvature of SNP. The adsorption experiments of lysozyme on SNP with different particle sizes proved that the saturated adsorption capacity of lysozyme increased with SNP sizes [28]. Therefore, it can be assumed that the addition of SNP plays a key role in protein aggregation, which improves the local concentration of lysozyme, and is beneficial to the growth of the 110-face.

In addition, as reported in previous work [28], lysozyme crystals could only be observed when the size of SNP reached 100 nm at a supersaturation of 4. Here in this work, lysozyme crystals were obtained with all sizes of SNP used at the same supersaturation, proving that the different properties of SNP could cause the difference in protein crystallization. Therefore, the mechanism of SNP inducing lysozyme crystallization needs to be further explored.

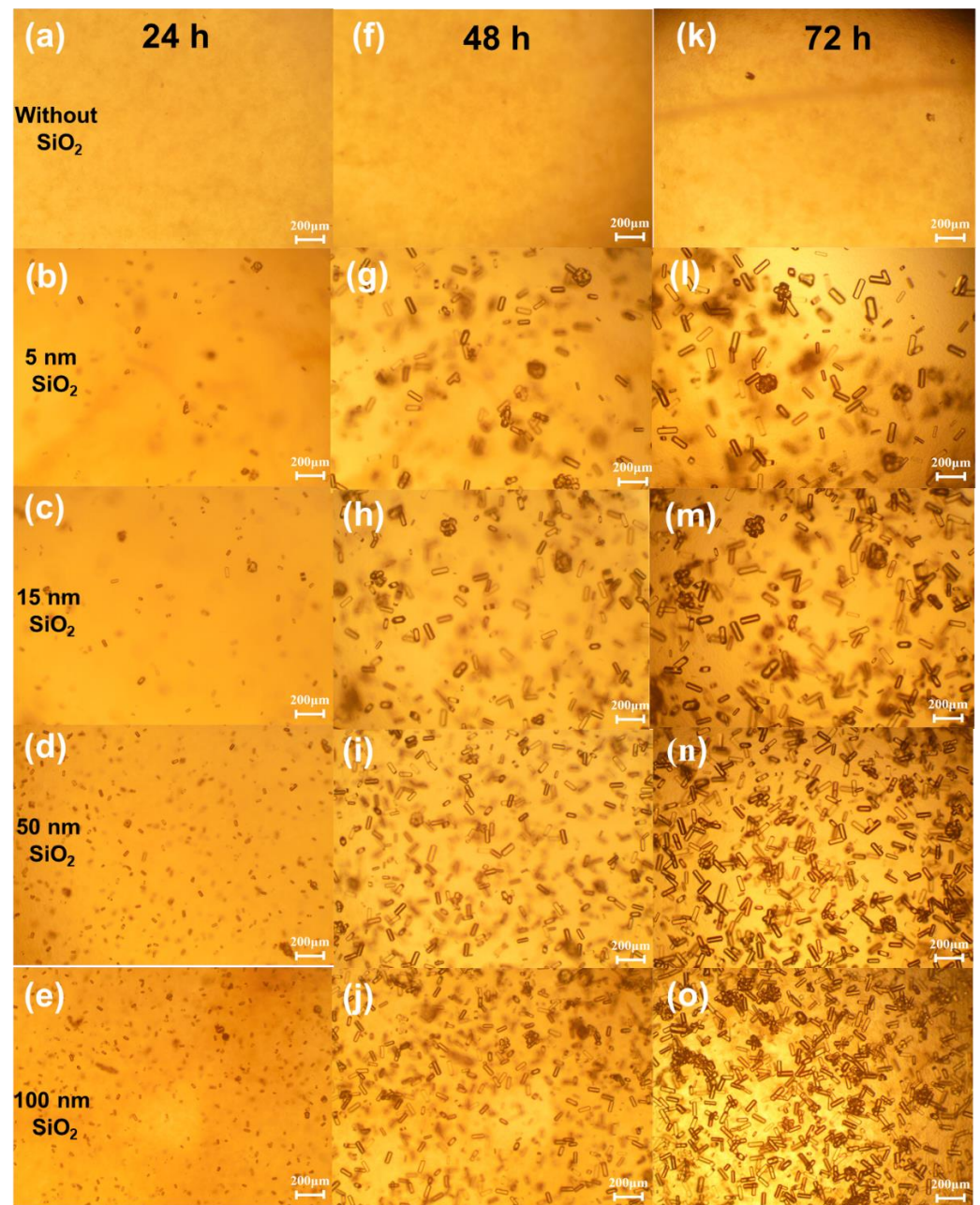


Figure 3. Microscopy photos of crystals obtained with SNP of different sizes. Conditions: 0.05 M, pH 4.5 sodium acetate buffer solution, 3 wt.% sodium chloride, 20 mg/mL lysozyme at 4 °C. Scale bar: 200 μm. (a): Crystal micrograph obtained under 24 h without SiO₂; (b): Crystal micrograph obtained at 24 h with 1 mg/mL 5 nm SiO₂; (c): Crystal micrograph obtained at 24 h with 1 mg/mL 15 nm SiO₂; (d): Crystal micrograph obtained at 24 h with 1 mg/mL 50 nm SiO₂; (e): Crystal micrograph obtained at 24 h with 1 mg/mL 100 nm SiO₂; (f): Crystal micrograph obtained under 48 h without SiO₂; (g): Crystal micrograph obtained at 48 h with 1 mg/mL 5 nm SiO₂; (h): Crystal micrograph obtained at 48 h with 1 mg/mL 15 nm SiO₂; (i): Crystal micrograph obtained at 48 h with 1 mg/mL 50 nm SiO₂; (j): Crystal micrograph obtained at 48 h with 1 mg/mL 100 nm SiO₂; (k): Crystal micrograph obtained under 72 h without SiO₂; (l): Crystal micrograph obtained at 72 h with 1 mg/mL 5 nm SiO₂; (m): Crystal micrograph obtained at 72 h with 1 mg/mL 15 nm SiO₂; (n): Crystal micrograph obtained at 72 h with 1 mg/mL 50 nm SiO₂; (o): Crystal micrograph obtained at 72 h with 1 mg/mL 100 nm SiO₂.

3.2. Zeta Potential of Lysozyme and SNP

Zeta potential measurements of SNP with different particle sizes and lysozyme were further performed. Figure 4a shows that SNP with different particle sizes was negatively charged. With the increase in the SNP size, the absolute value of the potential increased. Figure 4b shows that lysozyme was positively charged. Therefore, there should be an electrostatic interaction between SNP and lysozyme, increasing with the size of the SNP.

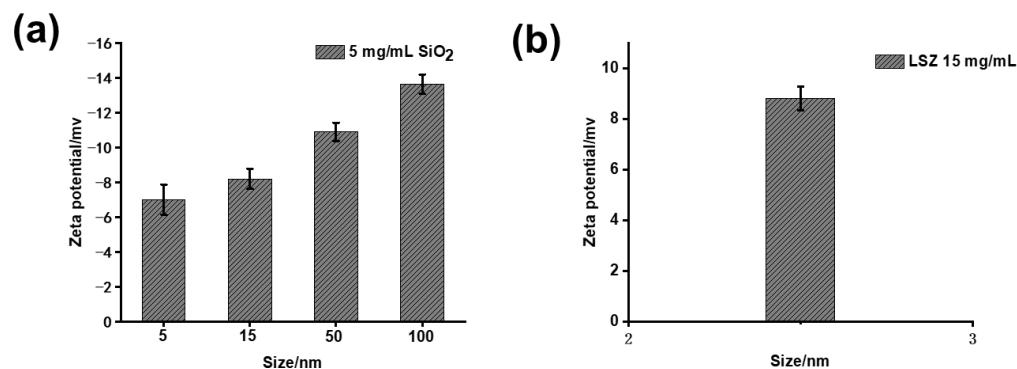


Figure 4. (a) Zeta potential of SNP with different particle sizes. (b) Zeta potential of lysozyme.

3.3. Effect of SNP Sizes on the UV Spectroscopy of Lysozyme

The UV spectra of lysozyme and SNP with different particle sizes were measured. As shown in Figure 5A, the spectrum exhibited absorbance peaks at 220 nm and 280 nm, respectively, which were caused by the presence of lysozyme. The UV spectrum of SNP was measured and showed no absorbance in the measured wavelength range (Figure S5). For the convenience of observation and discussion, the spectrum from 200 to 350 nm was intercepted (Figure 5B). An apparent increase in absorbance occurred with the addition of SNP at the same lysozyme concentration. According to the Lambert–Beer law, the absorbance value protein is in positive correlation with its concentration. Hence, it is assumed here that the increase in absorbance was mainly caused by an increase in local concentration of lysozyme. Due to the electrostatic interaction between lysozyme and SNP, lysozyme could be attracted and gathered at the surface of SNP, leading to an increase in local lysozyme concentration in solution. With the increase in SNP sizes, the interaction between lysozyme and SNP was enhanced, and the amount of lysozyme absorbed was further increased, resulting in a higher UV intensity.

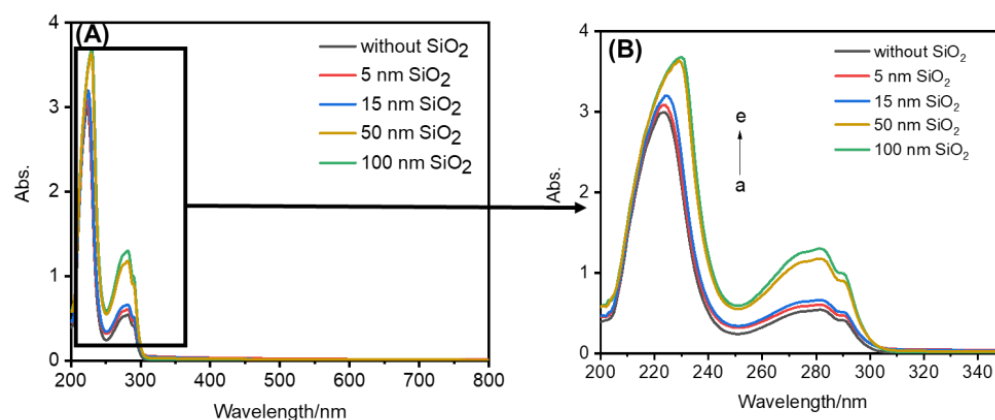


Figure 5. (A) UV spectrum from 200 nm to 800 nm. (B) UV spectrum from 200 nm to 350 nm. UV spectra of lysozyme solutions with and without SNP. From bottom to top: a, without SNP; b, 0.025 mg/mL 5 nm SNP; c, 0.025 mg/mL 15 nm SNP; d, 0.025 mg/mL 50 nm SNP; e, 0.025 mg/mL 100 nm SNP.

To verify the assumption above, the UV spectrum of pure lysozyme with different concentrations was measured (Figure S6). As shown in Figure S6, the UV absorbance increased with lysozyme concentration. The increasing trend and shape of the spectrum were consistent with Figure 5B. Hence, the presence of SNP can induce lysozyme aggregation and increase the local lysozyme concentration, which is more conducive to lysozyme crystallization.

3.4. Effect of SNP Sizes on the Fluorescence Spectroscopy Experiment of Lysozyme

Fluorescence experiments were carried out to further reveal the interaction between SNP and lysozyme. As shown in Figure 6, the fluorescence intensity of lysozyme increased after adding SNP of different sizes. For the same SNP size, the fluorescence intensity of lysozyme increased with the increase in SNP concentration. When the concentration of SNP was the same, the fluorescence intensity of lysozyme was higher after adding larger SNP.

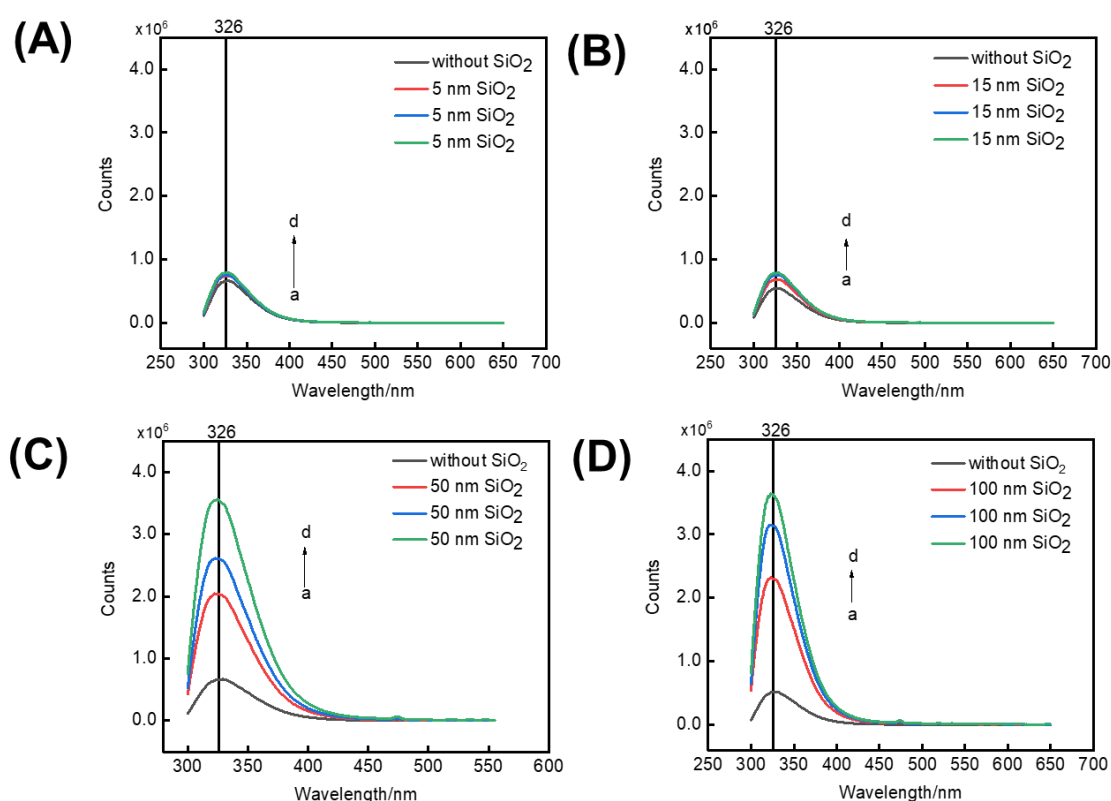


Figure 6. Fluorescence spectra of lysozyme solutions with and without SNP. (A) 5 nm SiO₂; (B) 15 nm SiO₂; (C) 50 nm SiO₂; (D) 100 nm SiO₂. From bottom to top: a, no SNP; b, 1 mg/mL; c, 2 mg/mL; d, 3 mg/mL.

There may be two possible reasons for the enhancement in fluorescence intensity [29,30]. Due to the aggregation of lysozyme caused by SNP, the probability of non-radiative relaxation of the excited state was reduced. Meanwhile, the contact probability between oxygen molecules with a quenching effect in water and chromogenic groups was reduced. As a result, the fluorescence intensity was enhanced.

3.5. Effect of SNP on Lysozyme Activity

In order to clarify the influence of the SNP–lysozyme interaction on lysozyme structure and function, the lysozyme activity and secondary structure were further determined. The activity test results are shown in Figure 7, and the results from circular dichroism are displayed in Figure S7. It can be found that the addition of SNP had almost no effect on the secondary structure and function of lysozyme.

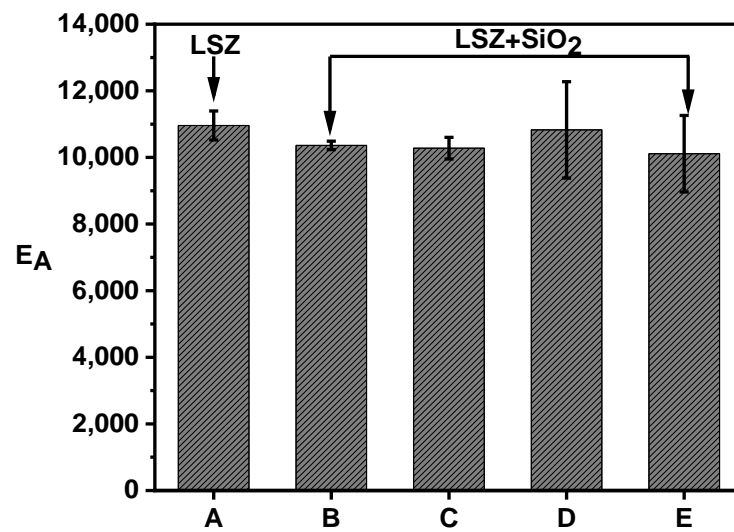


Figure 7. Effect of SNP on lysozyme activity. A: without SNP; B: 0.005 mg/mL 5 nm SiO₂; C: 0.005 mg/mL 15 nm SiO₂; D: 0.005 mg/mL 50 nm SiO₂; E: 0.005 mg/mL 100 nm SiO₂.

3.6. Mechanism of SNP-Induced Lysozyme Crystallization

Based on the results shown above, a mechanism of SNP-induced lysozyme crystallization is proposed and shown in Figure 8.

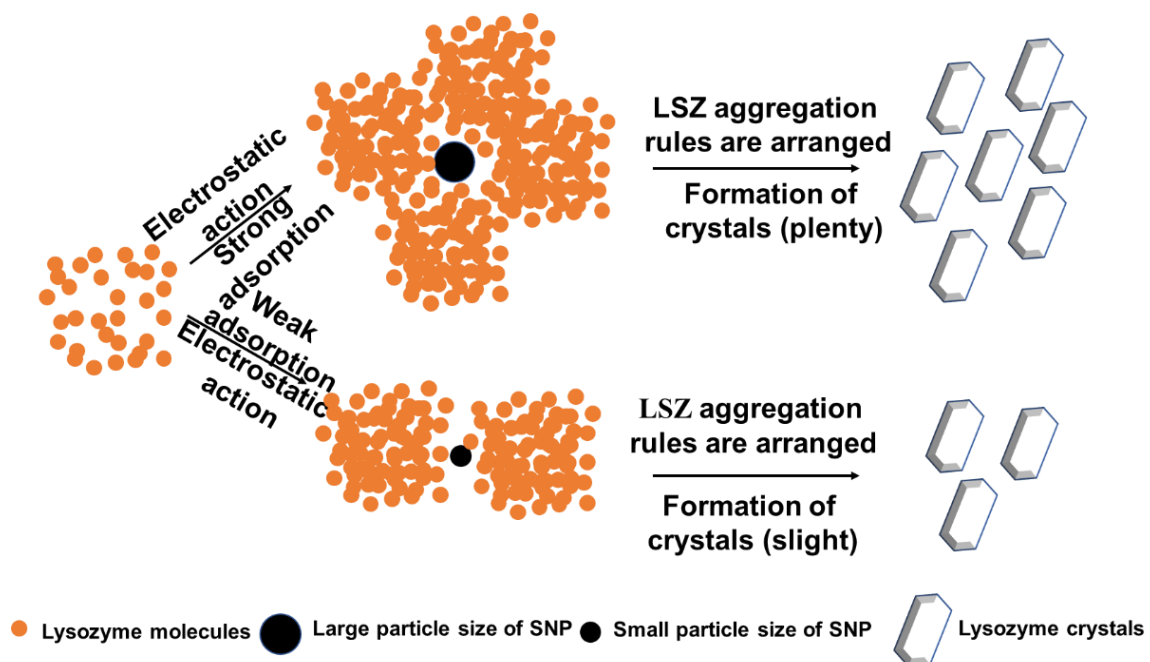


Figure 8. Mechanism of interaction between SNP with different particle sizes and lysozyme. (Note: the figure only shows the mechanism of a single SNP and lysozyme. There are multiple SNP and lysozymes in the specific crystallization process.)

Driven by electrostatic attraction, lysozyme adsorbs and aggregates on the surface of SNP, leading to an increase in lysozyme local concentration. As a result, the nucleation of lysozyme is easier when SNP is present. Moreover, the space occupied by each lysozyme molecule (asymmetric unit) in the crystal is a rectangular block with a size of $28.0 \text{ \AA} \times 28.0 \text{ \AA} \times 37 \text{ \AA}$ [31], which is smaller than the SNP sizes used here. It can be assumed that SNP only play the role of gathering lysozyme and do not participate in protein assembly. The initial nucleation conditions of lysozyme will not change by the addition of

SNP. With the increase in SNP size, the adsorption capacity of lysozyme increases, leading to a rise in the number of crystals.

4. Conclusions

The effects of SNP size on lysozyme crystallization were investigated. It was found that the morphological defects of lysozyme crystals were reduced after SNP addition. Further investigations showed that SNP can induce lysozyme aggregation and increase local supersaturation by electrostatic interaction, which increased with SNP size. As a result, lysozyme crystallizes easier with the addition of SNP, especially with SNP of larger size. Furthermore, the addition of SNP does not affect the secondary structure and function of lysozyme.

Supplementary Materials: The following supporting information can be downloaded at: <https://www.mdpi.com/article/10.3390/cryst12111623/s1>, Figure S1. Transmission electron microscopy images of SNP with different particle sizes. (a): 5 nm SiO₂, (b): 15 nm SiO₂, (c): 50 nm SiO₂, (d): 100 nm SiO₂; Figure S2. Crystal size distribution of 0.05 M, pH 4.5 sodium acetate buffer solution, 3 wt. % sodium chloride solution, 15 mg/mL lysozyme at 4 °C for 48 h. (a) 5 nm SiO₂, (b) 15 nm SiO₂, (c) 50 nm SiO₂, (d) 100 nm SiO₂; Figure S3. Crystal size distribution of 0.05 M, pH 4.5 sodium acetate buffer solution, 3 wt. % sodium chloride solution, 15 mg/mL lysozyme at 4 °C for 72 h. (a) 5 nm SiO₂, (b) 15 nm SiO₂, (c) 50 nm SiO₂, (d) 100 nm SiO₂; Figure S4. (a): Corresponding microscope image after mixing 1 mg/mL 50 nm SiO₂ and 20 mg/mL LSZ. (b): Corresponding microscope image after mixing 1 mg/mL 100 nm SiO₂ and 20 mg/mL LSZ; Figure S5. UV spectra of silica with different particle sizes; Figure S6. UV spectra of lysozyme at different concentrations; Figure S7. CD spectra of lysozyme in the presence and absence of SNP.

Author Contributions: Conceptualization, Y.Z. (Yuxiao Zhang), X.Y., F.H. and X.W. (Xiaoqiang Wang); methodology, Y.Z. (Yuxiao Zhang), X.Y., F.H. and X.W. (Xiaoqiang Wang); investigation, Y.Z. (Yuxiao Zhang), X.J., X.W. (Xia Wu), Y.M., S.L., K.L. and G.Z., Y.Z. (Yuyu Zhou); writing—original draft preparation, Y.Z. (Yuxiao Zhang); writing—review and editing, X.Y., F.H. and X.W. (Xiaoqiang Wang) All authors have read and agreed to the published version of the manuscript.

Funding: The work was supported by the National Natural Science Foundation of China (22178387).

Data Availability Statement: Not applicable.

Conflicts of Interest: The authors declare no conflict of interest.

References

1. Stevens, R.C. High-throughput protein crystallization. *Curr. Opin. Struct. Biol.* **2000**, *10*, 558–563. [CrossRef]
2. Dora, G.C. Crystal structure analysis: A primer. *Crystallogr. Rev.* **2011**, *17*, 157–160. [CrossRef]
3. Chayen, N.E. Turning protein crystallisation from an art into a science. *Curr. Opin. Struct. Biol.* **2004**, *14*, 577–583. [CrossRef] [PubMed]
4. Chayen, N.E.; Saridakis, E. Protein crystallization: From purified protein to diffraction-quality crystal. *Nat. Methods* **2008**, *5*, 147–153. [CrossRef] [PubMed]
5. Basu, S.K.; Govardhan, C.P.; Jung, C.W.; Margolin, A.L. Protein crystals for the delivery of biopharmaceuticals. *Expert Opin. Biol. Ther.* **2004**, *4*, 301–317. [CrossRef]
6. L'vov, P.E.; Umantsev, A.R. Two-Step Mechanism of Macromolecular Nucleation and Crystallization: Field Theory and Simulations. *Cryst. Growth Des.* **2020**, *21*, 366–382. [CrossRef]
7. Sear, R.P. Nucleation: Theory and applications to protein solutions and colloidal suspensions. *J. Phys. Condens. Matter* **2007**, *19*, 033101. [CrossRef]
8. Zhou, R.-B.; Cao, H.-L.; Zhang, C.-Y.; Yin, D.-C. A review on recent advances for nucleants and nucleation in protein crystallization. *CrystEngComm* **2017**, *19*, 1143–1155. [CrossRef]
9. Kordonskaya, Y.V.; Marchenkova, M.A.; Timofeev, V.I.; Dyakova, Y.A.; Pisarevsky, Y.V.; Kovalchuk, M.V. Precipitant ions influence on lysozyme oligomers stability investigated by molecular dynamics simulation at different temperatures. *J. Biomol. Struct. Dyn.* **2021**, *39*, 7223–7230. [CrossRef]
10. Kovalchuk, M.V.; Blagov, A.E.; Dyakova, Y.A.; Gruzinov, A.Y.; Marchenkova, M.A.; Peters, G.S.; Pisarevsky, Y.V.; Timofeev, V.I.; Volkov, V.V. Investigation of the initial crystallization stage in lysozyme solutions by small-angle X-ray scattering. *Cryst. Growth Des.* **2016**, *16*, 1792–1797. [CrossRef]

11. Kovalchuk, M.V.; Boikova, A.S.; Dyakova, Y.A.; Ilina, K.B.; Konarev, P.V.; Kryukova, A.E.; Marchenkova, M.A.; Pisarevsky, Y.V.; Timofeev, V.I. Pre-crystallization phase formation of thermolysin hexamers in solution close to crystallization conditions. *J. Biomol. Struct. Dyn.* **2019**, *37*, 3058–3064. [[CrossRef](#)]
12. Ko, S.; Kim, H.Y.; Choi, I.; Choe, J. Gold nanoparticles as nucleation-inducing reagents for protein crystallization. *Cryst. Growth Des.* **2017**, *17*, 497–503. [[CrossRef](#)]
13. Takeda, Y.; Mafuné, F. Induction of protein crystallization by platinum nanoparticles. *Chem. Phys. Lett.* **2016**, *647*, 181–184. [[CrossRef](#)]
14. Leese, H.S.; Govada, L.; Saridakis, E.; Khurshid, S.; Menzel, R.; Morishita, T.; Clancy, A.J.; White, E.R.; Chayen, N.E.; Shaffer, M.S. Reductively PEGylated carbon nanomaterials and their use to nucleate 3D protein crystals: A comparison of dimensionality. *Chem. Sci.* **2016**, *7*, 2916–2923. [[CrossRef](#)] [[PubMed](#)]
15. Delmas, T.; Roberts, M.M.; Heng, J.Y.Y. Nucleation and crystallization of lysozyme: Role of substrate surface chemistry and topography. *J. Adhes. Sci. Technol.* **2011**, *25*, 357–366. [[CrossRef](#)]
16. Lindberg, R.; Sjöblom, J.; Sundholm, G. Preparation of silica particles utilizing the sol-gel and the emulsion-gel processes. *Colloids Surf. A Physicochem. Eng. Asp.* **1995**, *99*, 79–88. [[CrossRef](#)]
17. Zhuravlev, L.T. Surface characterization of amorphous silica—A review of work from the former USSR. *Colloids Surf. A Physicochem. Eng. Asp.* **1993**, *74*, 71–90. [[CrossRef](#)]
18. Qian, R.; Ding, L.; Ju, H. Switchable fluorescent imaging of intracellular telomerase activity using telomerase-responsive mesoporous silica nanoparticle. *J. Am. Chem. Soc.* **2013**, *135*, 13282–13285. [[CrossRef](#)]
19. Ramanaviciene, A.; Zukiene, V.; Acaite, J.; Ramanavicius, A. Influence of caffeine on lysozyme activity in the blood serum of mice. *Acta Med. Litu.* **2002**, *9*, 241–244.
20. Yamazaki, T.; Kimura, Y.; Vekilov, P.G.; Furukawa, E.; Shirai, M.; Matsumoto, H.; Van Driessche, A.E.S.; Tsukamoto, K. Two types of amorphous protein particles facilitate crystal nucleation. *Proc. Natl. Acad. Sci. USA* **2017**, *114*, 2154–2159. [[CrossRef](#)]
21. Bhamidi, V.; Skrzypczak-Jankun, E.; Schall, C.A. Dependence of nucleation kinetics and crystal morphology of a model protein system on ionic strength. *J. Cryst. Growth* **2001**, *232*, 77–85. [[CrossRef](#)]
22. Cacioppo, E.; Pusey, M.L. The solubility of the tetragonal form of hen egg white lysozyme from pH 4.0 to 5.4. *J. Cryst. Growth* **1991**, *114*, 286–292. [[CrossRef](#)]
23. Tsekova, D.S. Formation and Growth of Tetragonal Lysozyme Crystals at Some Boundary Conditions. *Cryst. Growth Des.* **2009**, *9*, 1312–1317. [[CrossRef](#)]
24. Müller, C.; Ulrich, J. A more clear insight of the lysozyme crystal composition. *Cryst. Res. Technol.* **2011**, *46*, 646–650. [[CrossRef](#)]
25. Kang, M.; Lee, G.; Jang, K.; Jeong, D.W.; Lee, J.-O.; Kim, H.; Kim, Y.J. Graphene Quantum Dots as Nucleants for Protein Crystallization. *Cryst. Growth Des.* **2022**, *22*, 269–276. [[CrossRef](#)]
26. Forsythe, E.L.; Nadarajah, A.; Pusey, M.L. Growth of (101) faces of tetragonal lysozyme crystals: Measured growth-rate trends. *Acta Crystallogr. Sect. D Biol. Crystallogr.* **1999**, *55*, 1005–1011. [[CrossRef](#)] [[PubMed](#)]
27. Sun, X.; Feng, Z.; Zhang, L.; Hou, T.; Li, Y. The selective interaction between silica nanoparticles and enzymes from molecular dynamics simulations. *PLoS ONE* **2014**, *9*, e107696. [[CrossRef](#)] [[PubMed](#)]
28. Weichsel, U.; Segets, D.; Janeke, S.; Peukert, W. Enhanced nucleation of lysozyme using inorganic silica seed particles of different Sizes. *Cryst. Growth Des.* **2015**, *15*, 3582–3593. [[CrossRef](#)]
29. Luo, Z.; Yuan, X.; Yu, Y.; Zhang, Q.; Leong, D.T.; Lee, J.Y.; Xie, J. From aggregation-induced emission of Au (I)–thiolate complexes to ultrabright Au (0)@ Au (I)–thiolate core–shell nanoclusters. *J. Am. Chem. Soc.* **2012**, *134*, 16662–16670. [[CrossRef](#)]
30. Zhu, J.; He, K.; Dai, Z.; Gong, L.; Zhou, T.; Liang, H.; Liu, J. Self-assembly of luminescent gold nanoparticles with sensitive pH-stimulated structure transformation and emission response toward lysosome escape and intracellular imaging. *Anal. Chem.* **2019**, *91*, 8237–8243. [[CrossRef](#)]
31. Nadarajah, A.; Li, M.; Pusey, M.L. Growth mechanism of the (110) face of tetragonal lysozyme crystals. *Acta Crystallogr. Sect. D Biol. Crystallogr.* **1997**, *53*, 524–534. [[CrossRef](#)] [[PubMed](#)]